

Supplementary Material (ESI) for CrystEngComm
This journal is © The Royal Society of Chemistry

The electrochemical properties, nitrogen adsorption and photocatalytic activities of three 3D metal–organic frameworks bearing the rigid terphenyl tetracarboxylates ligands

Bao Mu, Chang-xia Li, Ming Song, Yan-li Ren, Ru-Dan Huang*

*Key Laboratory of Cluster Science of Ministry of Education, School of Chemistry,
Beijing Institute of Technology, Beijing, 100081, P. R. China*

ELECTRONIC SUPPLEMENTARY INFORMATION

Table S1. Selected bond distances (Å) and angles (deg) for complex 1.

Mn(1)–O(1)	2.243(4)	Mn(1)–O(4)#1	2.215(4)
Mn(1)–O(2)#2	2.188(3)	Mn(1)–O(2)#3	2.188(3)
Mn(1)–O(4)#4	2.215(4)	Mn(1)–O(1)#5	2.243(4)
O(1)–Mn(1)–O(4)#1	90.43(15)	O(1)–Mn(1)–O(2)#2	88.87(15)
O(1)–Mn(1)–O(2)#3	91.13(15)	O(1)–Mn(1)–O(4)#4	89.57(15)
O(1)–Mn(1)–O(1)#5	180	O(2)#2–Mn(1)–O(4)#1	82.77(17)
O(2)#3–Mn(1)–O(4)#1	97.23(17)	O(4)#1–Mn(1)–O(4)#4	180
O(1)#5–Mn(1)–O(4)#1	89.57(15)	O(2)#2–Mn(1)–O(2)#3	180
O(2)#2–Mn(1)–O(4)#4	97.23(17)	O(1)#5–Mn(1)–O(2)#2	91.13(15)
O(2)#3–Mn(1)–O(4)#4	82.77(17)	O(1)#5–Mn(1)–O(2)#3	88.87(15)
O(1)#5–Mn(1)–O(4)#4	90.43(15)		

Symmetry code for #1 1+x, -1+y, z; #2 1+x, y, z; #3 1-x, -y, 1-z; #4 1-x, 1-y, 1-z;

Table S2. Selected bond distances (Å) and angles (deg) for complex 2.

Ni1–O1	2.041(9)	Ni1–O10#7	2.071(9)
Ni1–O2	2.056(9)	Ni1–O8#2	2.091(8)
Ni1–O3	2.119(8)	Ni1–O11#3	2.075(9)
Ni2–O2W	2.083(9)	Ni2–O9#7	2.035(11)
Ni2–O3W	2.123(11)	Ni2–O1#1	2.082(8)
Ni2–O1	2.034(8)	Ni2–O4	1.995(9)
Ni3–O1W	2.089(9)	Ni3–O2#4	2.026(9)

* Corresponding author. *E-mail address:* huangrd@bit.edu.cn (R. D. Huang).

Ni3–O5	2.074(9)	Ni3–O12#5	2.052(10)
Ni3–O7	2.109(10)	Ni3–O2#6	2.016(8)
O1–Ni2–O2W	175.9(3)	O10#7–Ni1–O11#3	177.5(3)
O1–Ni2–O3W	93.2(4)	O8#2–Ni1–O11#3	86.0(3)
O1–Ni2–O4	100.0(3)	O1W–Ni3–O5	84.3(3)
O1–Ni2–O9#7	89.9(4)	O1W–Ni3–O7	85.8(4)
O1–Ni2–O1#1	87.8(3)	O1W–Ni3–O2#4	176.9(3)
O2W–Ni2–O3W	87.4(4)	O1W–Ni3–O12#5	90.9(4)
O2W–Ni2–O4	84.1(4)	O1W–Ni3–O2#6	96.4(3)
O2W–Ni2–O9#7	89.3(4)	O5–Ni3–O7	92.7(4)
O1#1–Ni2–O2W	88.1(3)	O2#4–Ni3–O5	92.8(3)
O3W–Ni2–O4	91.6(4)	O5–Ni3–O12#5	175.1(4)
O3W–Ni2–O9#7	175.4(4)	O2#6–Ni3–O5	92.8(3)
O1#1–Ni2–O3W	89.7(4)	O2#4–Ni3–O7	93.3(4)
O4–Ni2–O9#7	91.2(4)	O7–Ni3–O12#5	86.0(4)
O1#1–Ni2–O4	172.0(3)	O2#6–Ni3–O7	177.8(4)
O1#1–Ni2–O9#7	87.1(4)	O2#4–Ni3–O12#5	92.0(4)
O1–Ni1–O2	175.3(3)	O2#4–Ni3–O2#6	84.5(3)
O1–Ni1–O3	90.1(3)	O2#6–Ni3–O12#5	93.9(3)
O1–Ni1–O10#7	94.7(3)	O2–Ni1–O11#3	96.6(3)
O1–Ni1–O8#2	90.6(3)	O3–Ni1–O10#7	93.1(3)
O1–Ni1–O11#3	83.9(4)	O3–Ni1–O8#2	174.9(3)
O2–Ni1–O3	85.3(3)	O3–Ni1–O11#3	89.0(3)
O2–Ni1–O10#7	85.0(3)	O8#2–Ni1–O10	91.9(3)
O2–Ni1–O8#2	94.1(3)		

Symmetry code for #1 2–x, –y, 1–z; #2 1+x, y, z; #3 2–x, –y, –z; #4 –1+x, y, z; #5 –1+x, 1+y, z; #6 1–x, 1–y, –z; #7 1–x, 1–y, 1–z

Table S3. Selected bond distances (Å) and angles (deg) for complex **3**.

Zn(1)–O(1)#1	2.005(2)	Zn(1)–O(3)#3	1.950(3)
Zn(1)–O(3)#2	1.950(3)	Zn(1)–O(1)	2.005(2)
O(1)–Zn(1)–O(2)	53.28(7)	O(1)–Zn(1)–O(3)#3	102.59(10)
O(1)–Zn(1)–O(1)#1	97.98(8)	O(1)–Zn(1)–O(2)#1	150.89(8)
O(1)–Zn(1)–O(3)#2	99.94(9)	O(2)–Zn(1)–O(3)#3	84.23(9)

O(1)#1–Zn(1)–O(2)	150.89(8)	O(2)–Zn(1)–O(2)#1	155.75(6)
O(2)–Zn(1)–O(3)#2	88.60(9)	O(1)#1–Zn(1)–O(3)#3	99.94(9)
O(2)#1–Zn(1)–O(3)#3	88.60(9)	O(3)#2–Zn(1)–O(3)#3	145.38(9)
O(1)#1–Zn(1)–O(2)#1	53.28(7)	O(1)#1–Zn(1)–O(3)#2	102.59(10)
O(2)#1–Zn(1)–O(3)#2	84.23(9)		

Symmetry code for #1 $-x, y, -1/2-z$; #2 $-x, -y, -z$; #3 $x, -y, -1/2+z$

Table S4. Hydrogen-bonding geometry (Å, °) for complex **2**.

D–H···A	D–H	H···A	D···A	D–H···A
O(1W)–H(1WA)···O(4W)	0.85	2.09	2.914(15)	164
O(2W)–H(2WB)···O(8) ^a	0.85	2.15	2.923(13)	152
O(3W)–H(3WB)···O(8) ^a	0.85	2.20	2.981(12)	153
O(4W)–H(4WB)···O(11) ^a	0.85	2.02	2.864(15)	170

Symmetry code for (a) $1-x, 1-y, -z$

Table S5. Hydrogen-bonding geometry (Å, °) for complex **3**.

D–H···A	D–H	H···A	D···A	D–H···A
N(2)–H(2A)···O(4) ^{--H(3)}	0.90	2.02	2.823(3)	147
N(2)–H(2B)···O(5) ^a	0.90	2.00	2.841(4)	156

Symmetry code for (a) $x, 1-y, 1/2+z$

Preparation of complexes 1–2 bulk-modified carbon paste electrode

The **2**–CPE was prepared as follows: the mixture of 0.5 g graphite powder and 0.031 g complex **2** were ground using agate mortar and pestle for half an hour. 0.15 mL paraffin oil was added into the mixture and stirred uniformly, which was packed into a 3 mm inner diameter and 0.7 cm length glass tube. The electrical contact was built through the copper stick. The other CPE was made with complex **1** by the similar method.

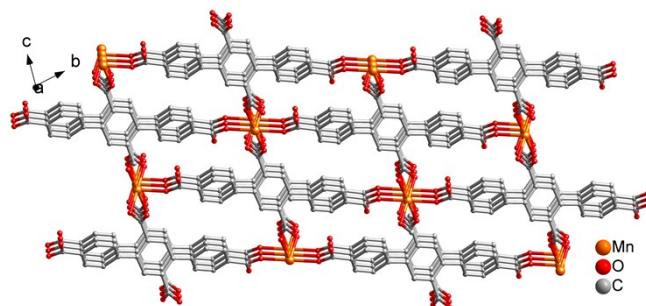


Fig. S1. The 3D framework in complex 1.

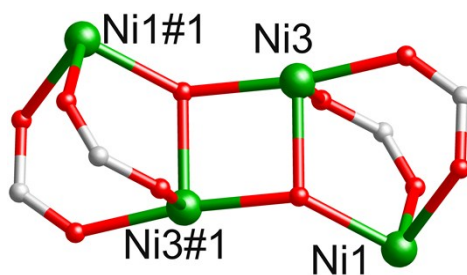


Fig. S2. The Ni₃-O quadrangle from (Ni₃)₂-Ni₁ unit in complex 2 (#1 $-x, 2-y, 1-z$).

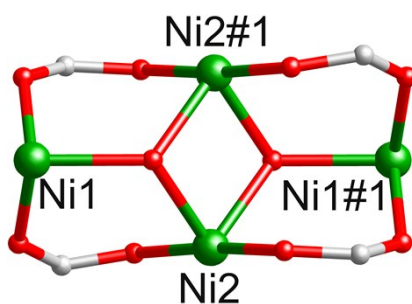


Fig. S3. The Ni₂-O rhombus from (Ni₂)₂-Ni₁ unit in complex 2 (#1 $2-x, -y, -z$).

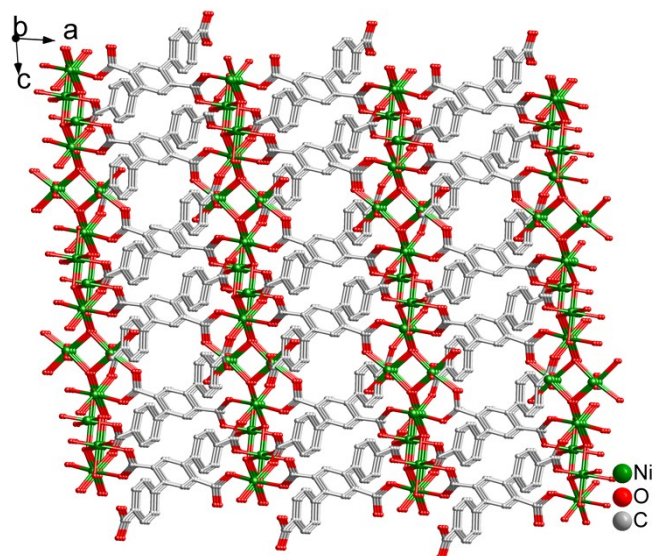


Fig. S4. The 3D framework in complex 2.

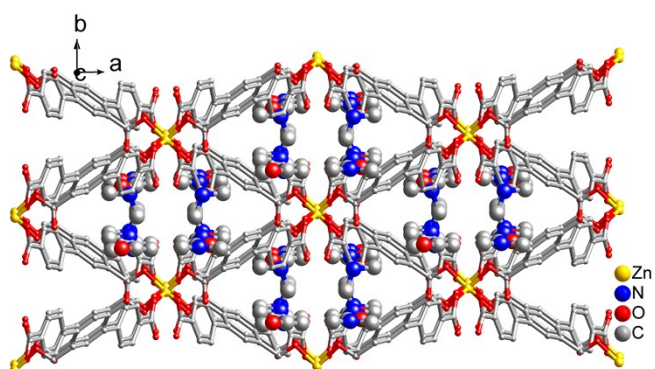


Fig. S5. The 3D framework containing the counterions $(\text{CH}_3)_2\text{NH}_2^+$ and solvent DMF molecules in complex 3.

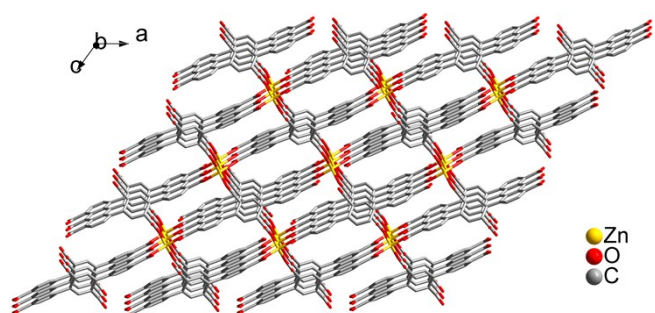


Fig. S6. The 3D framework without the counterions $(\text{CH}_3)_2\text{NH}_2^+$ and solvent DMF molecules in complex 3.

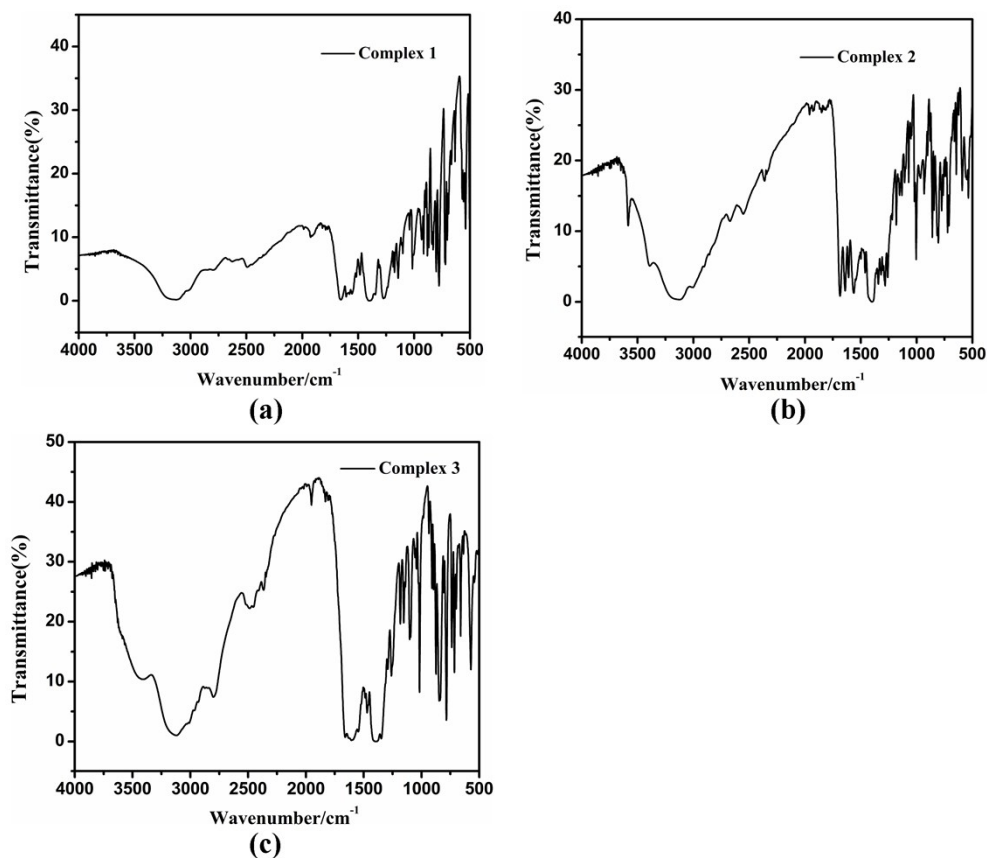


Fig. S7. The IR spectra of complexes **1–3**.

Powder X-ray diffraction analyses

Fig. S8 presents the powder X-ray diffraction (PXRD) peaks of simulated and experimental patterns to prove the purities for complexes **1–3**. The experimental patterns correlate with the relevant positions of the simulated patterns, indicating the phase purity of the title complexes. The slight differences of intensities between the simulated and experimental patterns may be due to the preferred orientation of crystals.

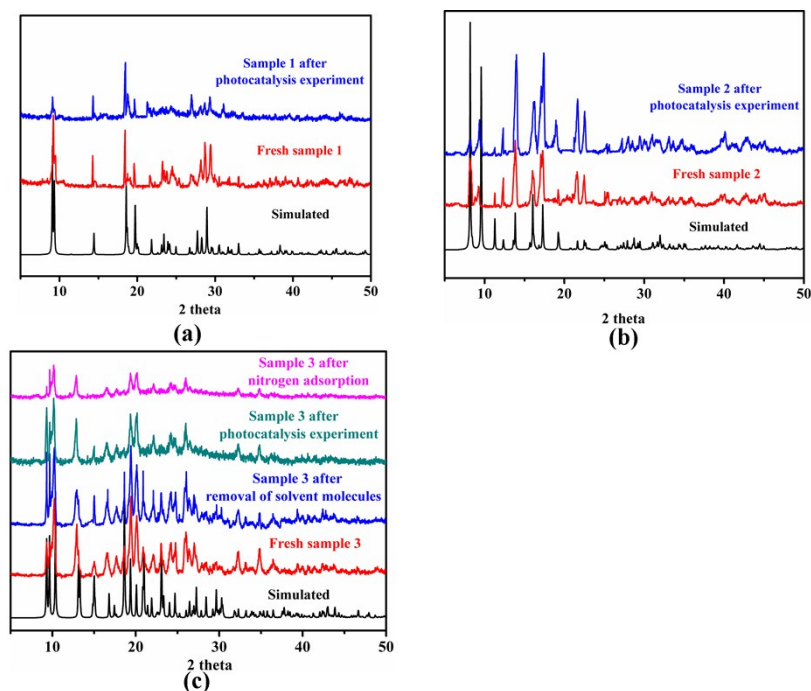


Fig. S8. The simulated, fresh samples, sample after the removal of solvent molecules, samples after photocatalytic experiments and sample after nitrogen adsorption powder X-ray diffraction patterns for complexes **1–3**.

Thermogravimetric analyses

The thermal stabilities of complexes **1–3** were measured in the temperature range of 30–800 °C under nitrogen atmosphere with the heating rate of 10 °C min⁻¹. The thermogravimetric (TG) analyses reveal that complex **1** shows one weight loss step, while complexes **2–3** display two weight loss steps (Fig. S9). For complex **1**, the weight loss of 84.99% can be due to the decomposition of **H₂L** ligands (calc. 84.55%). The final residual component MnO is about 15.01% (calc. 15.45%). For complex **2**, in the first step, the weight loss is 3.97%, corresponding to the loss of lattice water molecules (calc. 3.80%) from 30 °C to 185 °C. The second weight loss from the decomposition of **L** ligands and the loss of the coordinated water molecules and the hydroxyl groups is 66.04% between 370 °C to 490 °C (calc. 64.71%). The final remaining weight is 29.99%, which may be attributed to NiO (calc. 31.49%). For complex **3**, the first step lost the solvent DMF molecules of 22.39% from 30 °C to 240 °C (calc. 20.70%). The second weight loss process of 65.23% is between 350 °C

to 580 °C, which may be assigned to the decomposition of **L** ligands and counterions $(\text{CH}_3)_2\text{NH}_2^+$ (calc. 67.77%). The final products of 12.38% may be metal oxide ZnO (calc. 11.53%).

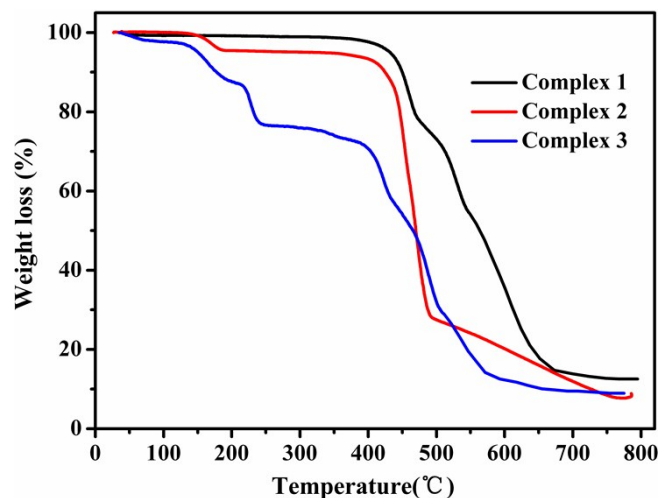


Fig. S9. The TG curves of complexes 1–3.

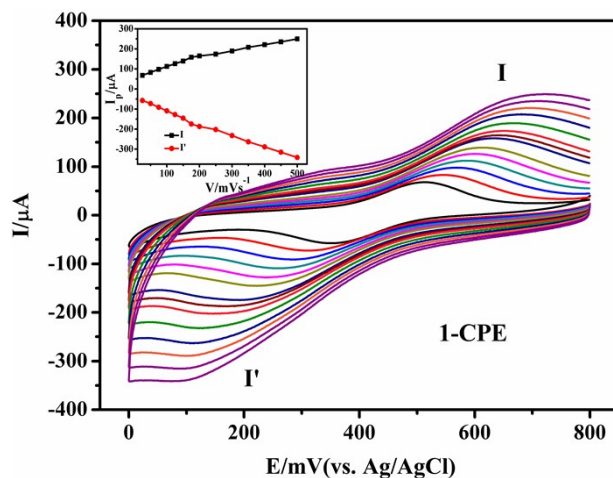


Fig. S10. Cyclic voltammograms of the 1-CPE in 0.01 M H_2SO_4 + 0.5 M Na_2SO_4 aqueous solution at different scan rates (from inner to outer: 25, 50, 75, 100, 125, 150, 175, 200, 250, 300, 350, 400, 450, 500 $\text{mV}\cdot\text{s}^{-1}$). The inset shows the plots of the anodic and cathodic peak currents against scan rates.

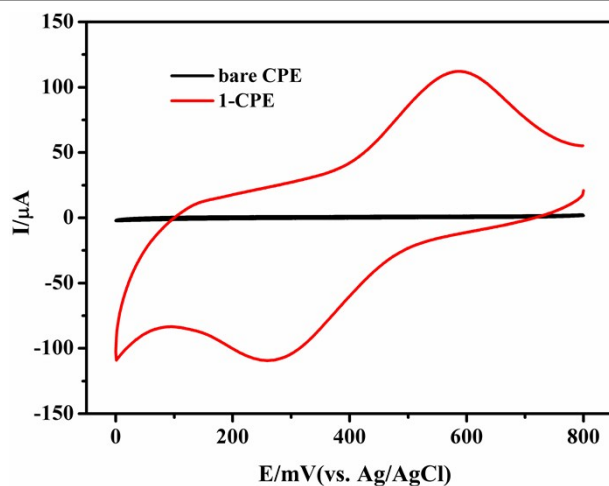


Fig. S11. Cyclic voltammogram of 1-CPE (0 to 800 mV for 1-CPE) in 0.01 M $\text{H}_2\text{SO}_4 + 0.5$ M Na_2SO_4 aqueous solution for complex 1. Scan rate: 100 mVs^{-1} .

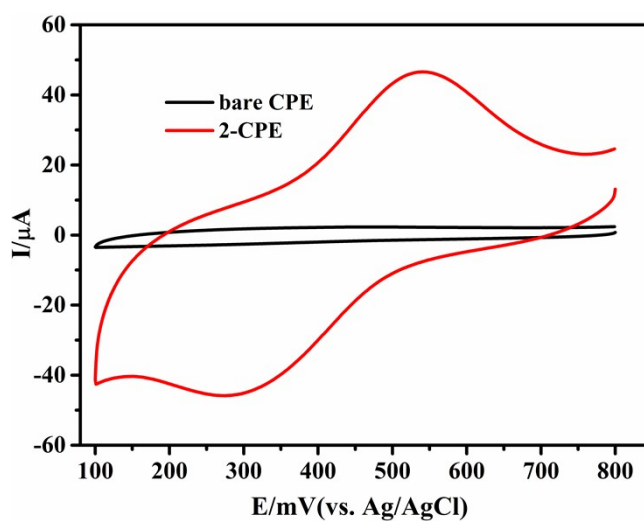


Fig. S12. Cyclic voltammogram of 2-CPE (100 to 800 mV for 2-CPE) in 0.01 M $\text{H}_2\text{SO}_4 + 0.5$ M Na_2SO_4 aqueous solution for complex 2. Scan rate: 100 mVs^{-1} .

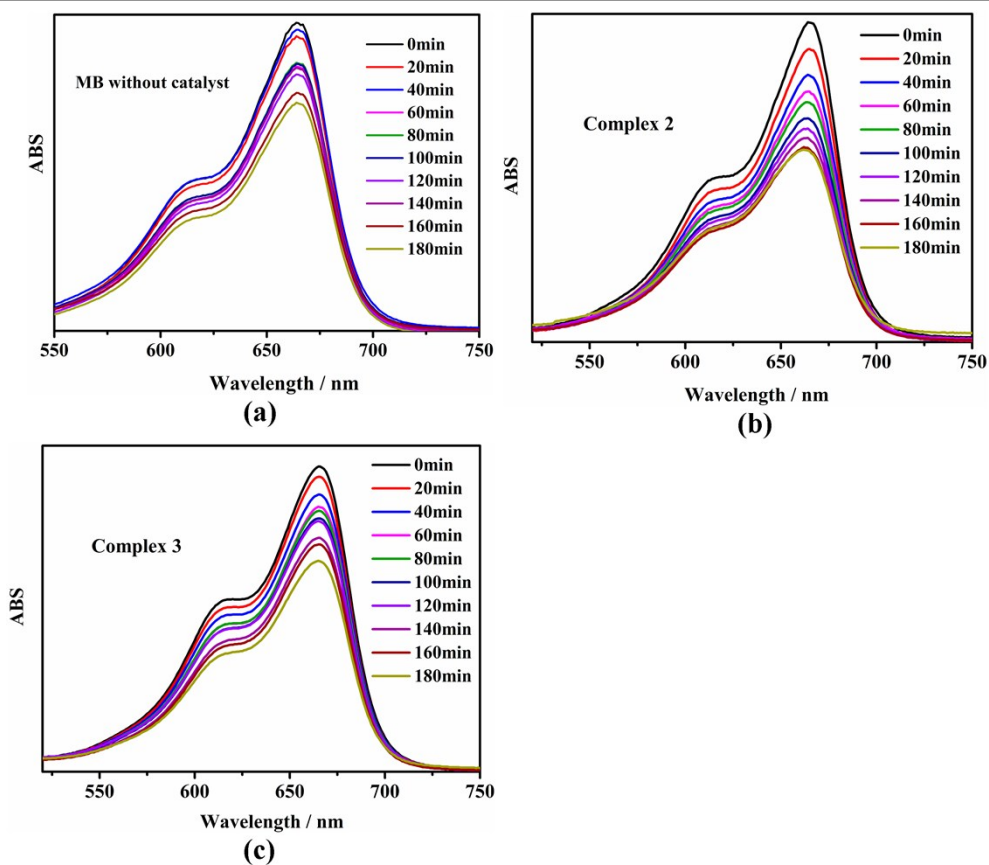


Fig. S13. Absorption spectra of the MB solution during the decomposition reaction under the visible light irradiation with the presences of complexes 2–3 and no crystal in the same conditions.